

Imaging of Common Solid Organ and Bowel Torsion in the Emergency Department

Andres R. Ayoub¹
James T. Lee

OBJECTIVE. This article will discuss the most common forms of torsion encountered in the emergency department.

CONCLUSION. Torsion refers to the twisting of an object about its axis and represents the pathophysiologic mechanism underlying an important group of disorders affecting both the bowel and the solid organs of the abdomen and pelvis. Although these disorders typically present with the acute onset of pain, clinical findings are often nonspecific, with imaging playing a key role in diagnosis. Missed or delayed diagnosis may result in complications, such as ischemia; end-organ loss; and, in some cases, death. Therefore, it is critical to have a thorough understanding of the pathophysiology and imaging findings of these entities to avoid the morbidity and mortality associated with a missed or delayed diagnosis.

Torsion refers to the twisting of an object about its axis and is the pathophysiologic mechanism underlying an important group of disorders affecting both the bowel and the solid organs of the abdomen and pelvis. Torsion may be partial or complete and can be constant or intermittent. These conditions typically present with acute onset of pain, the character and severity of which often reflect the underlying degree and constancy of the torsion. When untreated, torsion may progress to ischemia and infarction resulting in end-organ loss and, in some cases, death. Given nonspecific clinical features and the possibility of organ salvage with early diagnosis and intervention, imaging plays a vital role in patient management and outcome. Ultrasound is the typical initial imaging test for suspected testicular and ovarian torsion, whereas CT is the primary modality to evaluate for suspected bowel torsion.

A traditional system-based approach often addresses torsion of the bowel and solid organs separately. However, considering these entities based on a common pathophysiologic mechanism may prompt recognition of imaging findings and complications, aid in understanding of predisposing factors, and facilitate use of a systematic approach to imaging evaluation (Appendix 1).

The commonly proposed pathophysiologic mechanism of torsion includes initial obstruction

of lymphatic flow within the end organ, resulting in interstitial edema and organ enlargement; subsequent increase in pressure leading to venous outflow obstruction; and progression to arterial inflow compromise with resultant ischemia or infarction.

It follows naturally from the pathophysiology that torsion results in abnormalities of the end organ and the supplying vascular pedicle, both of which can be detected at imaging (Table 1). Imaging of the vascular pedicle focuses on identifying morphologic changes as a result of the twist, whereas the affected organ may show one or more of the following: morphologic changes, abnormal position or lie, or altered vascularity.

Although most torsions require prompt surgical intervention, there are forms of torsion that are not organ threatening and are treated nonsurgically. However, because these disorders are a source of acute pain and mimic surgically treated conditions, recognition is important to avoid unnecessary invasive treatment. This article will discuss the most common forms of torsion encountered in the emergency department.

Testicular Torsion

Testicular torsion results from twisting of the spermatic cord, which contains, among other structures, the testicular, cremasteric, and deferential arteries; pampiniform plexuses; and lymphatic vessels. This results in

Keywords: bowel, ovary, testicle, torsion, volvulus

DOI:10.2214/AJR.13.12279

Received November 21, 2013; accepted after revision February 5, 2014.

Presented at the 2013 annual meeting of ARRS, Washington, DC.

¹Both authors: Department of Radiology, University of Kentucky, 800 Rose St, Rm HX316, Lexington, KY 40536-2410. Address correspondence to A. R. Ayoub (andres.ayoub@uky.edu).

This article is available for credit.

WEB

This is a web exclusive article.

AJR 2014; 203:W470–W481

0361–803X/14/2035–W470

© American Roentgen Ray Society

Imaging of Solid Organ and Bowel Torsion

alterations of testicular blood flow and patients typically present with acute-onset testicular pain. Surgical detorsion is the definitive treatment of testicular torsion.

Two forms of testicular torsion have been described on the basis of surgical findings: extravaginal and intravaginal. Extravaginal torsion, accounting for a minority of cases (10%), is torsion proximal to the attachment to the tunica vaginalis (outside the tunica vaginalis) [1]. This occurs in neonates who typically present at birth with an infarcted necrotic testicle [2, 3]. Intravaginal torsion accounts for the majority of cases and is torsion distal to the attachment of the tunica vaginalis (within the tunica vaginalis) [4]. Although it may occur at any age, intravaginal torsion is most common between 12–18 years [5, 6]. Predisposing factors include a long narrow mesentery or an anomalous reflection of the tunica vaginalis [7]. The bell-clapper deformity is a high attachment of the tunica vaginalis such that it extends completely around the testicle and epididymis to envelop a length of the spermatic cord (Fig. 1). This allows the testis to rotate within the tunica vaginalis, analogous to a clapper inside a bell [7].

Ultrasound is the imaging modality of choice for evaluation of acute-onset scrotal pain, and gray-scale and Doppler assessment of both the testicle and vascular pedicle (spermatic cord) should be performed. Imaging findings and outcome are dependent on the degree and duration of torsion. The salvage rate drops from nearly 100% within the first 6 hours of symptom onset to approximately 20% after 12 hours, making early detection of torsion the primary objective [8]. Doppler evaluation is key to the early diagnosis of testicular torsion because alterations in vascular flow are detected before gray-scale findings [9]. Torsion is not an “all or none” phenomenon with regard to blood flow—that is, flow does not have to be absent in the setting of torsion. Experimental studies have shown that 720° of torsion is required to occlude the testicular artery [5].

With complete absence of flow, diagnosis is typically straightforward, and a definitive diagnosis of complete testicular torsion can be made when blood flow is detected on the normal side but is absent on the affected side (Fig. 2). However, when torsion is incomplete, flow may be present, although diminished, on the affected side [10]. Meticulous comparison of testicular blood flow is the key in this setting, and the “buddy shot” (a side-by-side comparison of the testes ob-

TABLE 1: Imaging Features of End Organ and Pedicle

Parameter	End Organ	Pedicle
Bowel	Abnormal position	Whirl sign
	Altered orientation	X-marks-the-spot sign
	Ischemic findings	Split-wall sign
Ovary	Abnormal position	Twisted vascular pedicle
	Morphologic changes	Whirlpool sign
	Altered vascularity	
Testicle	Altered position or lie	Twisted vascular pedicle
	Morphologic changes	Whirlpool sign
	Altered vascularity	

tained with color Doppler imaging) nicely highlights asymmetric blood flow (Fig. 2). Spectral Doppler sonography may be helpful in the diagnosis of partial torsion. Although the resistive index may be altered in the affected testicle, there is a broad range of overlap with normal resistive indexes. A defined cutoff value for the resistive index (above or below which a diagnosis can be confidently made) has not been validated. Variability of the Doppler waveform compared with the contralateral testicle (either increased or decreased amplitude arterial waveform), variability within the same testicle, and reversal of diastolic flow have been described as indirect clues that suggest the diagnosis of partial testicular torsion [11].

Gray-scale findings are not specific for testicular torsion [12] and may be normal early in the course of disease. Testicular enlargement and alterations in echotexture and echogenicity develop as ischemia progresses. Regions of infarction appear hypoechoic relative to normal parenchyma, whereas a mixed pattern of echogenicity results from hemorrhagic infarction secondary to hyperechoic blood [10]. Once such gray-scale changes have occurred, the testicle is likely nonviable (Fig. 2). Conversely, normal testicular echotexture is highly predictive of testicular viability [13].

Assessment of the vascular pedicle (spermatic cord) is also essential in imaging evaluation of acute scrotal pain because it represents direct imaging of the site of torsion. This is particularly useful in evaluation of incomplete torsion, in which blood flow alterations may be subtle, and of intermittent testicular torsion, a clinical syndrome defined by a history of unilateral sudden-onset scrotal pain of short duration that resolves spontaneously [14]. Abrupt changes in spermatic cord size, course, or echotexture can be detected

on sonography. The finding of a spiral twist of the cord has been found to have high sensitivity and specificity for torsion [15, 16] (Fig. 3). The finding of rotation of the cord structures, detected by moving the transducer in a downward direction perpendicular to the axis of the cord, has been described as the whirlpool sign [17]. Additional imaging features may include abnormal testicular position with an elevated transversely oriented testicle, scrotal wall thickening, and reactive hydrocele.

Torsion of the Testicular Appendage

Patients with torsion of the testicular appendage present with the acute onset of scrotal pain, and it is difficult to differentiate from testicular torsion on the basis of clinical findings alone. Distinction is important because this entity is treated nonsurgically, with attention to pain management. Testicular appendage torsion typically occurs in boys 7–14 years old [18]. The classic physical examination finding is the “blue dot” sign, a nodule on the superior aspect of the testis exhibiting bluish discoloration through the skin [19].

The testicular appendages are remnants of mesonephric and paramesonephric ducts that consist of vascularized connective tissue. The sessile nature of these structures predisposes to torsion [20]. Although there are five testicular appendages, the appendix testis accounts for up to 95% of cases of torsion [18]. The appendix testis, a paramesonephric duct remnant, is attached to the upper pole of the testis in the groove between the testis and the epididymis. When visualized, a normal appendix testis appears as an ovoid structure approximately 5 mm in length that is typically isoechoic to the testis but may occasionally be cystic [18]. Typical sonographic findings of a torsed appendix testis include an enlarged (> 5–7 mm) spherical mass separate from the epididymal head

TABLE 2: Testicular and Ovarian Torsion Sonographic Findings

Parameter	Gray-Scale Ultrasound	Doppler Ultrasound
Testicular torsion	Limited diagnostic value <ul style="list-style-type: none"> • No abnormality may be evident • If gray-scale abnormalities present, testicle not likely viable Useful for assessment of testicular viability	Key in diagnosis <p>May show absent or asymmetrically decreased vascularity</p>
Ovarian torsion	Key in diagnosis <ul style="list-style-type: none"> • Enlarged ovary is most consistent finding • Torsion unlikely with normal size and gray-scale appearance • Ovary often round or globular in shape and heterogeneous in echotexture 	Limited diagnostic value <ul style="list-style-type: none"> • There may be no detectable flow in normal ovary • Asymmetric flow is common and depends on phase of menstrual cycle • Dual ovarian arterial blood supply

showing variable echogenicity (Fig. 4). Doppler evaluation shows lack of internal vascularity, although peripheral hyperemia may be present [7] (Fig. 4). A reactive hydrocele and skin thickening may also be identified.

Ovarian Torsion

Ovarian torsion results from twisting of the ovary about the suspensory ligament, which contains the ovarian artery and vein, lymphatics, and nerves. The term “adnexal torsion” is inclusive of the ovary, fallopian tube, or both (Fig. 5). Although ovarian torsion may occur at any age, it is most common during the reproductive years, with up to 20% of cases occurring during pregnancy [21]. Symptoms are nonspecific but often include acute onset of sharp lower abdominal pain and tenderness with possible palpable mass and peritoneal signs. Treatment is surgical with laparoscopic detorsion and possible oophoropexy or oophorectomy.

There are multiple proposed predisposing factors. Ovarian torsion is commonly associated with ovarian masses, which are thought to predispose the ovary to swing on its vascular pedicle (Fig. 5). Masses typically associated with torsion include large follicular cysts, hemorrhagic cysts, benign mature cystic teratomas (the most common tumor predisposed to ovarian torsion), and cystadenomas [22–24]. The risk appears to be size dependent because it is rare to identify torsion in cysts smaller than 5 cm [25]. Torsion of a normal ovary is unusual but is more common in adolescents and has been proposed to be secondary to hypermobility of pelvic ligaments, fallopian tube, and mesosalpinx [26, 27]. Conversely, ovarian torsion is uncommonly associated with pelvic inflammatory disease, endometriosis, and malignant neoplasms, which are thought to result in diminished ovarian mobility from adhesions [28–30].

Ultrasound is the typical first-line imaging modality in evaluation of lower abdominal pain in a young female patient. Gray-scale findings are of critical importance because it is unusual to have ovarian torsion with a morphologically normal ovary. In fact, ovarian enlargement (> 4 cm or > 22 mL) is the most constant finding in ovarian torsion [22]. Other morphologic changes include peripherally located follicles (string of pearls sign) and a heterogeneous ovarian stroma [21] (Fig. 5). A coexistent ovarian mass may also be present (Figs. 5 and 6).

Doppler findings, on the other hand, are highly variable and often misleading, limiting the value of this modality in diagnosis of ovarian torsion. Variability in flow patterns detected on Doppler imaging are based on the degree of vascular compromise (partial vs complete) and are complicated by the dual ovarian blood supply (via both the ovarian artery and the adnexal branch of the uterine artery), which may enable preservation of arterial flow in the face of ovarian torsion [31]. The classic Doppler finding of absent arterial inflow is not found in all cases (Fig. 7). In fact, the most frequent Doppler finding is either decreased or absent venous flow [22] (Fig. 7).

Identification of a twisted vascular pedicle may also aid in diagnosis. The twisted pedicle is typically identified as an echogenic round or beaked mass with multiple concentric hypoechoic stripes [23]. Visualization of the coiled vessels with the twisted pedicle on color Doppler sonography has been described as the whirlpool sign [18]. A comparison of the utility of gray-scale and Doppler imaging in the assessment of testicular and ovarian torsion is provided in Table 2.

CT findings of ovarian torsion include midline ovarian displacement, uterine deviation toward the involved ovary, adnexal enlargement with or without an ovarian mass, and

inflammatory changes in the pelvic fat [32, 33]. The twisted vascular pedicle may also be identified as a mass between the uterus and ovary (Fig. 6). Free fluid may be detected with ultrasound or CT but is a nonspecific finding.

Volvulus

Torsion of the bowel, which results in obstruction, is referred to as “volvulus.” Clinical findings in cases of intestinal volvulus are nonspecific and include abdominal pain, nausea, vomiting, and constipation. Diagnosis is often not suspected until identified on imaging studies, typically radiography or CT. Prompt recognition of imaging findings is critical to avoid ischemia, infarction, and perforation, which may occur with delayed diagnosis.

Gastric Volvulus

Typical presenting symptoms of gastric volvulus include epigastric pain, nausea, and vomiting. The presence of sudden-onset epigastric pain, intractable retching, and inability to pass an enteric tube has been described with gastric volvulus and is referred to as the Borchardt triad.

Predisposing factors include laxity in the supporting gastric ligaments (primary volvulus) and anatomic abnormalities not primarily related to the gastric attachments that allow space for gastric movement (secondary volvulus). In adults, the most commonly associated anatomic abnormality is a paraesophageal hernia, whereas in children, a congenital diaphragmatic hernia is most common [34, 35]. Posttraumatic diaphragmatic hernia and left hemidiaphragm paralysis or eventration are additional associated predisposing anatomic abnormalities [36].

Predisposing factors include laxity in the supporting gastric ligaments and abnormal space for gastric movement, such as with posttraumatic diaphragmatic hernia, para-

esophageal hernia, congenital diaphragmatic defect, or left hemidiaphragm paralysis or eventration [36]. Twisting of the stomach may occur around its long axis (organoaxial), its short axis (mesenteroaxial), or a combination of both (complex or mixed) [37]. Organoaxial volvulus is the more common of the two basic subtypes. A gastric volvulus may be complete ($> 180^\circ$), resulting in gastric outlet obstruction, or incomplete (partial, $< 180^\circ$) without obstruction. Emergent surgical repair is the treatment of choice for acute gastric volvulus whereas endoscopic reduction may be indicated in patients who are not surgical candidates.

Identification of the orientation of the gastric components is the key to imaging diagnosis. Organoaxial volvulus occurs when the stomach rotates about the luminal (long) axis. This results in a "reversed" orientation of the greater and lesser curvatures (Fig. 8) with the greater curvature displaced cranially and the lesser curvature caudally. This orientation can be detected on both CT and upper gastrointestinal examinations. Luminal contrast material or gastric contents usually distend the stomach with minimal passage into the small bowel when a complete (180° or more) volvulus is present [38]. Strangulation is more common with this type of volvulus, occurring in up to 30% of cases [34, 39]. With incomplete volvulus and lack of signs or symptoms of obstruction, it is more accurate to describe the stomach as being in an organoaxial position.

Mesenteroaxial volvulus refers to gastric rotation around the gastrohepatic ligament (short axis) resulting in displacement of the antrum above the gastroesophageal junction (Fig. 9). A gastric volvulus with both organoaxial and mesenteroaxial components is referred to as a "complex" or "mixed" volvulus.

Midgut Volvulus

Midgut volvulus refers to a twist of the small bowel about a shortened mesenteric root. Although it typically presents acutely in the first month of life with bilious vomiting, it has become more frequently recognized in adults and is the most common cause of small-bowel obstruction in adults with malrotation [40]. Patients may present acutely with symptoms of small-bowel obstruction, such as abdominal pain, nausea, and vomiting, or, if the volvulus spontaneously reduces, patients may experience chronic intermittent abdominal pain [36].

The major predisposing factor for midgut volvulus is malrotation, in which there is abnormal fixation of the small mesentery. Imaging manifestations of malrotation include ectopic small-bowel position (with most of the small bowel in the right abdomen), abnormal location of the ligament of Treitz, typically below and to the right of the left L1 pedicle (the ligament of Treitz is normally located at or to the left of the L1 pedicle), and a reversed relationship of the superior mesenteric artery and vein (the proximal superior mesenteric artery located to the right of the superior mesenteric vein) [36, 40].

The abnormal mesenteric fixation present in malrotation produces a shortened mesenteric root, which predisposes the small bowel to twist on its mesentery resulting in midgut volvulus. In the presence of a midgut volvulus, the twisted segment of small bowel has a characteristic corkscrew appearance at fluoroscopy [41]. On CT, a swirling of vessels in the mesenteric root has been described at the site of the mesenteric twist [40, 41].

Colonic Volvulus

The sigmoid colon is the most common site of colonic volvulus, accounting for approximately 60–75% of all cases [42]. It is generally considered to be an acquired condition, occurring with an increased incidence in patients with chronic constipation and a redundant sigmoid colon. Chronic illness, prolonged hospitalization or institutionalization, pregnancy, high-fiber diets, and Chagas disease are all conditions associated with sigmoid volvulus. Often, intraluminal reduction via colonoscope or contrast enema can be successfully performed. Surgical intervention is required in patients who show signs and symptoms of bowel ischemia or when intraluminal reduction is not successful [42].

The cecum accounts for approximately 25–40% of colonic volvulus [42]. Predisposing factors must include both abnormal peritoneal fixation (resulting in a mobile cecum) and a fixed point of restriction (such as a mass or adhesion) to provide a fulcrum for rotation. There are two types of cecal volvulus: axial torsion and loop type [43] (Fig. 10). Axial torsion results from either clockwise or counterclockwise rotation of the cecum about its long axis, with the cecum remaining in the right lower quadrant. Loop-type torsion combines both the longitudinal rotation of the axial type with an inversion. This results in cranial displacement, with the cecum typically positioned in the left upper quadrant [44].

Controversy remains with regard to classification of a dilated ectopic cecum located in the midabdomen. Considered by some a variant of volvulus, this finding is often described as a cecal bascule, referring to the anterior, cranial, and medial folding of the cecum on the ascending colon without a mesenteric twist. Others consider this configuration a form of a focal adynamic ileus. In either case, if cecal bascule is suspected in the setting of bowel obstruction, surgical consultation is warranted because it is generally accepted that this condition may lead to bowel ischemia and perforation as a result of a flap-valve occlusion at the site of flexion [45]. Cecopexy is typically the treatment of choice for uncomplicated cecal volvulus given the low success rate and high incidence of recurrence with colonoscopic reduction. Surgical resection is required in cases of ischemia or perforation.

Sigmoid and cecal volvulus share many imaging findings. Differing from volvulus in other locations, sigmoid and to a lesser extent cecal volvulus may have diagnostic radiographic findings. An inverted U-shaped segment of colon resembling a coffee-bean is classically associated with sigmoid volvulus but can be seen with cecal volvulus as well [36, 46] (Fig. 11). The "northern exposure" sign refers to cephalic extension of sigmoid in relation to transverse colon on supine abdominal radiographs in sigmoid volvulus [47]. Conventional radiographic findings for cecal volvulus are less specific; gas-distended bowel with haustral markings directed toward the left upper quadrant is the classic radiographic finding [36].

The beak sign, which describes an abrupt tapering of the bowel lumen or contrast column at the site of torsion, can be detected on both CT and contrast enema examinations in sigmoid or cecal volvulus. Multiple CT findings of the mesenteric twist have been described: whirl sign, "X-marks-the-spot" sign, and "split wall" sign [46] (Fig. 12). The whirl sign describes the swirling appearance of collapsed bowel and its associated mesenteric vessels at the site of mesenteric rotation [48, 49]. The location of the whirl sign has been shown to be an accurate finding in discriminating between cecal and sigmoid volvulus, with a location to the right of the midline indicative of a cecal volvulus and a location in the midline or to the left of midline indicative of a sigmoid volvulus [50]. The X-marks-the-spot sign describes two crossing transition points projecting from a single location identified at CT on serial ax-

ial images, whereas the split wall sign refers to the apparent split in a single loop of incompletely twisted bowel caused by invagination of mesenteric fat [46] (Fig. 12). Proximal obstruction may be present in both types of colonic volvuli.

Complications of volvulus, such as ischemia, infarction, and perforation, may also be identified at imaging and should be actively sought out by the radiologist. Bowel-wall thickening and luminal dilatation have been described as the most common findings of bowel ischemia [51]. Alterations in the enhancement pattern of the bowel wall also occur, including both abnormalities in the degree and morphology of enhancement. Ischemic bowel may show either decreased or absent enhancement or increased enhancement. Increased enhancement has been associated with both hyperemia and hyperperfusion of the bowel wall [52]. Although not specific for ischemia, the target sign is a pattern of altered enhancement that has been described and refers to alternating layers of high and low attenuation within the thickened bowel wall, thought to result from submucosal edema [53]. Intramural gas and portal venous or mesenteric gas suggest a breakdown of the compromised bowel mucosa and are more specific imaging signs of ischemia [52]. Free intraperitoneal or retroperitoneal gas may occur and is indicative of perforation.

Epiploic Appendagitis

Epiploic appendages are fat-containing structures concentrated in the cecum and sigmoid colon that project from the tenia coli, usually measuring about 1–2 cm in thickness and 5 cm in length. The vascular stalk of the appendage passes through a narrow pedicle predisposing this structure to torsion [54, 55]. Although most torsions of the gastrointestinal tract require immediate intervention, epiploic appendagitis is managed nonoperatively with pain control measures. Signs and symptoms are nonspecific and can mimic other acute abdominal processes depending on the location of torsion. CT plays a critical role in the diagnosis, characteristically showing an oval fat-containing lesion with a thin rim of high attenuation that abuts the colon wall and is surrounded by inflammation (Fig. 13). The colonic wall is typically spared. The central dot sign, a punctate central focus of high attenuation within the fat-containing mass, is thought to represent a thrombosed vein and is a characteristic finding [54, 55].

Omental Infarct

Omental infarction is a rare cause of acute abdominal pain often presenting with pain localized to the right upper or lower quadrant as a result of vascular compromise of the greater omentum [56]. Although symptoms may mimic those of surgical diseases, such as appendicitis and acute cholecystitis, treatment of omental infarction is nonsurgical using supportive measures, making accurate diagnosis essential.

Postulated mechanisms include omental torsion or venous insufficiency [57]. Primary omental torsion has been proposed to be due to congenital variations, such as a bifid omentum or congenital attachment abnormalities. Secondary torsion, the more common subtype, is thought to occur as a result of abnormal attachment of the omentum to pathologic foci, such as scars or masses [56, 58]. The greater length and mobility of the omentum in the right abdomen relative to the left abdomen has been proposed to account for the increased frequency of right-sided infarction [56].

CT findings include a heterogeneous fat-containing nonenhancing omental mass most often located either anterior to the transverse colon or anteromedial to the ascending colon [56]. Omental infarct can be differentiated from epiploic appendagitis by its lack of a hyperattenuating ring, absence of a central dot sign, larger size (maximal diameter > 5 cm), and location (omental infarction typically occurs adjacent to the transverse or right colon, whereas epiploic appendagitis usually occurs adjacent to the sigmoid and descending colon) [4, 56]. When infarction results from torsion, swirling of the vessels is often visible within the omentum [59]. Similar to epiploic appendagitis, in omental infarct, the adjacent colon is usually spared.

Conclusion

Disorders resulting from torsion represent an important category of pathology. They present acutely and are typically imaged in the emergency setting. Prompt recognition and treatment of these disorders are required to avoid potential ischemic complications. Although in a traditional system-based approach torsions of the bowel and solid organs are often discussed separately, it is useful to consider these entities together on the basis of their common pathophysiologic mechanism. This approach may facilitate use of a systematic approach to image interpretation and aid in the recognition of imaging findings and complications.

Acknowledgment

We thank Tom Dolan, senior medical illustrator and multimedia developer, University of Kentucky, for the medical illustrations in this article.

References

1. Backhouse KM. Embryology of testicular descent and maldescent. *Urol Clin North Am* 1982; 9:315–325
2. Hawtrey CE. Assessment of acute scrotal symptoms and findings: a clinician's dilemma. *Urol Clin North Am* 1998; 25:715–723, x.
3. Zerlin JM, DiPietro MA, Grignon A, Shea D. Testicular infarction in the newborn: ultrasound findings. *Pediatr Radiol* 1990; 20:329–330
4. Lubner MG, Simard ML, Peterson CM, Bhalla S, Pickhardt PJ, Menias CO. Emergent and nonemergent nonbowel torsion: spectrum of imaging and clinical findings. *RadioGraphics* 2013; 33:155–173
5. Herbener TE. Ultrasound in the assessment of the acute scrotum. *J Clin Ultrasound* 1996; 24:405–421
6. Tumeh SS, Benson CB, Richie JP. Acute diseases of the scrotum. *Semin Ultrasound CT MR* 1991; 12:115–130
7. Dogra VS, Gottlieb RH, Oka M, Rubens DJ. Sonography of the scrotum. *Radiology* 2003; 227:18–36
8. Patriquin HB, Yazbeck S, Trinh B, et al. Testicular torsion in infants and children: diagnosis with Doppler sonography. *Radiology* 1993; 188:781–785
9. Lerner RM, Mevorach RA, Hulbert WC, Rabinowitz R. Color Doppler US in the evaluation of acute scrotal disease. *Radiology* 1990; 176:355–358
10. Ragheb D, Higgins JL Jr. Ultrasonography of the scrotum: technique, anatomy, and pathologic entities. *J Ultrasound Med* 2002; 21:171–185
11. Cassar S, Bhatt S, Paltiel HJ, Dogra VS. Role of spectral Doppler sonography in the evaluation of partial testicular torsion. *J Ultrasound Med* 2008; 27:1629–1638
12. Horstman WG. Scrotal imaging. *Urol Clin North Am* 1997; 24:653–671
13. Middleton WD, Middleton MA, Dierks M, Keetch D, Dierks S. Sonographic prediction of viability in testicular torsion: preliminary observations. *J Ultrasound Med* 1997; 16:23–27; quiz, 29–30
14. Creagh TA, McDermott TE, McLean PA, Walsh A. Intermittent torsion of the testis. *BMJ* 1988; 297:525–526
15. Baud C, Veyrac C, Couture A, Ferran JL. Spiral twist of the spermatic cord: a reliable sign of testicular torsion. *Pediatr Radiol* 1998; 28:950–954
16. Kalfa N, Veyrac C, Baud C, Couture A, Averous M, Galifer RB. Ultrasonography of the spermatic cord in children with testicular torsion: impact on the surgical strategy. *J Urol* 2004; 172(4 Pt 2):1692–1695; discussion, 1695
17. Vijayaraghavan SB. Sonographic whirlpool sign in ovarian torsion. *J Ultrasound Med* 2004;

Imaging of Solid Organ and Bowel Torsion

- 23:1643–1649; quiz, 50–51
18. Dogra V, Bhatt S. Acute painful scrotum. *Radiol Clin North Am* 2004; 42:349–363
19. Skoglund RW, McRoberts JW, Ragde H. Torsion of testicular appendages: presentation of 43 new cases and a collective review. *J Urol* 1970; 104:598–600
20. Aso C, Enriquez G, Fite M, et al. Gray-scale and color Doppler sonography of scrotal disorders in children: an update. *RadioGraphics* 2005; 25:1197–1214
21. Chang HC, Bhatt S, Dogra VS. Pearls and pitfalls in diagnosis of ovarian torsion. *RadioGraphics* 2008; 28:1355–1368
22. Albayram F, Hamper UM. Ovarian and adnexal torsion: spectrum of sonographic findings with pathologic correlation. *J Ultrasound Med* 2001; 20:1083–1089
23. Lee EJ, Kwon HC, Joo HJ, Suh JH, Fleischer AC. Diagnosis of ovarian torsion with color Doppler sonography: depiction of twisted vascular pedicle. *J Ultrasound Med* 1998; 17:83–89
24. Stark JE, Siegel MJ. Ovarian torsion in prepubertal and pubertal girls: sonographic findings. *AJR* 1994; 163:1479–1482
25. Warner BW, Kuhn JC, Barr LL. Conservative management of large ovarian cysts in children: the value of serial pelvic ultrasonography. *Surgery* 1992; 112:749–755
26. Breech LL, Hillard PJ. Adnexal torsion in pediatric and adolescent girls. *Curr Opin Obstet Gynecol* 2005; 17:483–489
27. Mordehai J, Mares AJ, Barki Y, Finaly R, Meizner I. Torsion of uterine adnexa in neonates and children: a report of 20 cases. *J Pediatr Surg* 1991; 26:1195–1199
28. Oelsner G, Shashar D. Adnexal torsion. *Clin Obstet Gynecol* 2006; 49:459–463
29. Warner MA, Fleischer AC, Edell SL, et al. Uterine adnexal torsion: sonographic findings. *Radiology* 1985; 154:773–775
30. Graif M, Shalev J, Strauss S, Engelberg S, Mashlach S, Itzhak Y. Torsion of the ovary: sonographic features. *AJR* 1984; 143:1331–1334
31. Rosado WM Jr, Trambert MA, Gosink BB, Pretorius DH. Adnexal torsion: diagnosis by using Doppler sonography. *AJR* 1992; 159:1251–1253
32. Bennett GL, Slywotzky CM, Giovannelli G. Gynecologic causes of acute pelvic pain: spectrum of CT findings. *RadioGraphics* 2002; 22:785–801
33. Rha SE, Byun JY, Jung SE, et al. CT and MR imaging features of adnexal torsion. *RadioGraphics* 2002; 22:283–294
34. Rashid F, Thangarajah T, Mulvey D, Larvin M, Iftikhar SY. A review article on gastric volvulus: a challenge to diagnosis and management. *Int J Surg* 2010; 8:18–24
35. Darani A, Mendoza-Sagaon M, Reinberg O. Gastric volvulus in children. *J Pediatr Surg* 2005; 40:855–858
36. Peterson CM, Anderson JS, Hara AK, Carenza JW, Menias CO. Volvulus of the gastrointestinal tract: appearances at multimodality imaging. *Radiology* 2009; 29:1281–1293
37. Federle MP, Jeffrey RB Jr, Woodward PJ, Borhani A. *Diagnostic imaging: abdomen*. Salt Lake City, UT: Amirsys, 2004
38. Shivanand G, Seema S, Srivastava DN, et al. Gastric volvulus: acute and chronic presentation. *Clin Imaging* 2003; 27:265–268
39. Wasselle JA, Norman J. Acute gastric volvulus: pathogenesis, diagnosis, and treatment. *Am J Gastroenterol* 1993; 88:1780–1784
40. Bernstein SM, Russ PD. Midgut volvulus: a rare cause of acute abdomen in an adult patient. *AJR* 1998; 171:639–641
41. McAlister WH, Kronemer KA. Emergency gastrointestinal radiology of the newborn. *Radiol Clin North Am* 1996; 34:819–844
42. Jones IT, Fazio VW. Colonic volvulus: etiology and management. *Dig Dis* 1989; 7:203–209
43. Delabrousse E, Sarlieve P, Sailley N, Aubry S, Kastler BA. Cecal volvulus: CT findings and correlation with pathophysiology. *Emerg Radiol* 2007; 14:411–415
44. Moore CJ, Corl FM, Fishman EK. CT of cecal volvulus: unraveling the image. *AJR* 2001; 177:95–98
45. Bobroff LM, Messinger NH, Subbarao K, Beneventano TC. The cecal bascule. *Am J Roentgenol Radium Ther Nucl Med* 1972; 115:249–252
46. Levsky JM, Den EI, DuBrow RA, Wolf EL, Rozenblit AM. CT findings of sigmoid volvulus. *AJR* 2010; 194:136–143
47. Javors BR, Baker SR, Miller JA. The northern exposure sign: a newly described finding in sigmoid volvulus. *AJR* 1999; 173:571–574
48. Frank AJ, Goffner LB, Fruauff AA, Losada RA. Cecal volvulus: the CT whirl sign. *Abdom Imaging* 1993; 18:288–289
49. Shaff MI, Himmelfarb E, Sacks GA, Burks DD, Kulkarni MV. The whirl sign: a CT finding in volvulus of the large bowel. *J Comput Assist Tomogr* 1985; 9:410
50. Macari M, Spieler B, Babb J, Pachter HL. Can the location of the CT whirl sign assist in differentiating sigmoid from caecal volvulus? *Clin Radiol* 2011; 66:112–117
51. Lee R, Tung HK, Tung PH, Cheung SC, Chan FL. CT in acute mesenteric ischaemia. *Clin Radiol* 2003; 58:279–287
52. Wiesner W, Khurana B, Ji H, Ros PR. CT of acute bowel ischemia. *Radiology* 2003; 226:635–650
53. Rha SE, Ha HK, Lee SH, et al. CT and MR imaging findings of bowel ischemia from various primary causes. *RadioGraphics* 2000; 20:29–42
54. Almeida AT, Melao L, Viamonte B, Cunha R, Pereira JM. Epiploic appendagitis: an entity frequently unknown to clinicians—diagnostic imaging, pitfalls, and look-alikes. *AJR* 2009; 193:1243–1251
55. Singh AK, Gervais DA, Hahn PF, Sagar P, Mueller PR, Novelline RA. Acute epiploic appendagitis and its mimics. *RadioGraphics* 2005; 25:1521–1534
56. Singh AK, Gervais DA, Lee P, et al. Omental infarct: CT imaging features. *Abdom Imaging* 2006; 31:549–554
57. Karak PK, Millmond SH, Neumann D, Yamase HT, Ramsby G. Omental infarction: report of three cases and review of the literature. *Abdom Imaging* 1998; 23:96–98
58. Kim J, Kim Y, Cho OK, et al. Omental torsion: CT features. *Abdom Imaging* 2004; 29:502–504
59. Kamaya A, Federle MP, Desser TS. Imaging manifestations of abdominal fat necrosis and its mimics. *RadioGraphics* 2011; 31:2021–2034

APPENDIX I: Predisposing Factors for Torsion of Bowel and Solid Organs

Attachment of pedicle to body wall

- Lack of fixation (bell-clapper deformity, testicular torsion)
- Malrotation (cecal volvulus)

Pedicle

- Redundant mesentery (sigmoid volvulus)
- Lax pelvic ligaments and fallopian tubes (proposed risk factor in ovarian torsion)

Organ

- Mass serving as lead point (ovarian torsion)
- Abnormal motility and bowel dilatation (cecal volvulus)

(Figures start on next page)

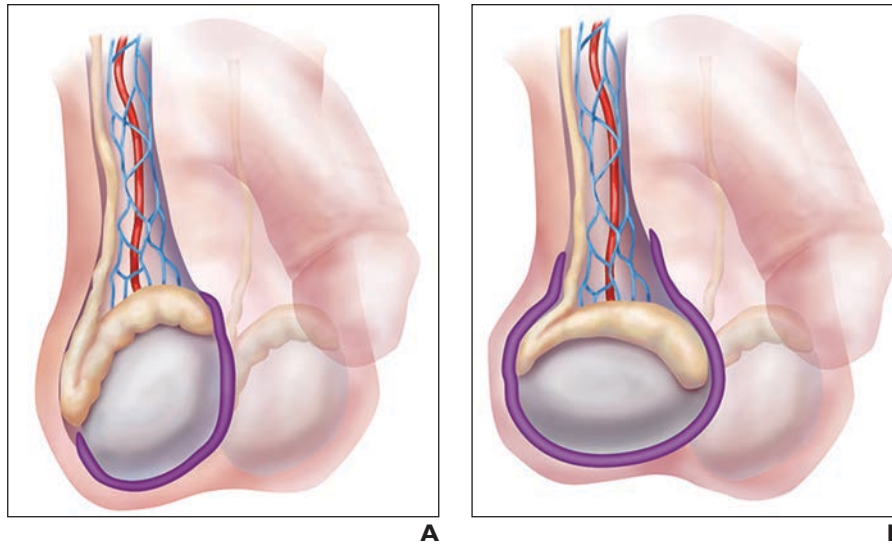


Fig. 1—Tunica vaginalis.

A, Drawing shows normal reflection of tunica vaginalis. Note parietal and visceral layers of tunica vaginalis (*purple*) join at posterolateral testis, where tunica attaches to scrotal wall.

B, Drawing shows bell-clapper deformity. High attachment of tunica vaginalis (*purple*) encircles epididymis, testis, and distal spermatic cord.

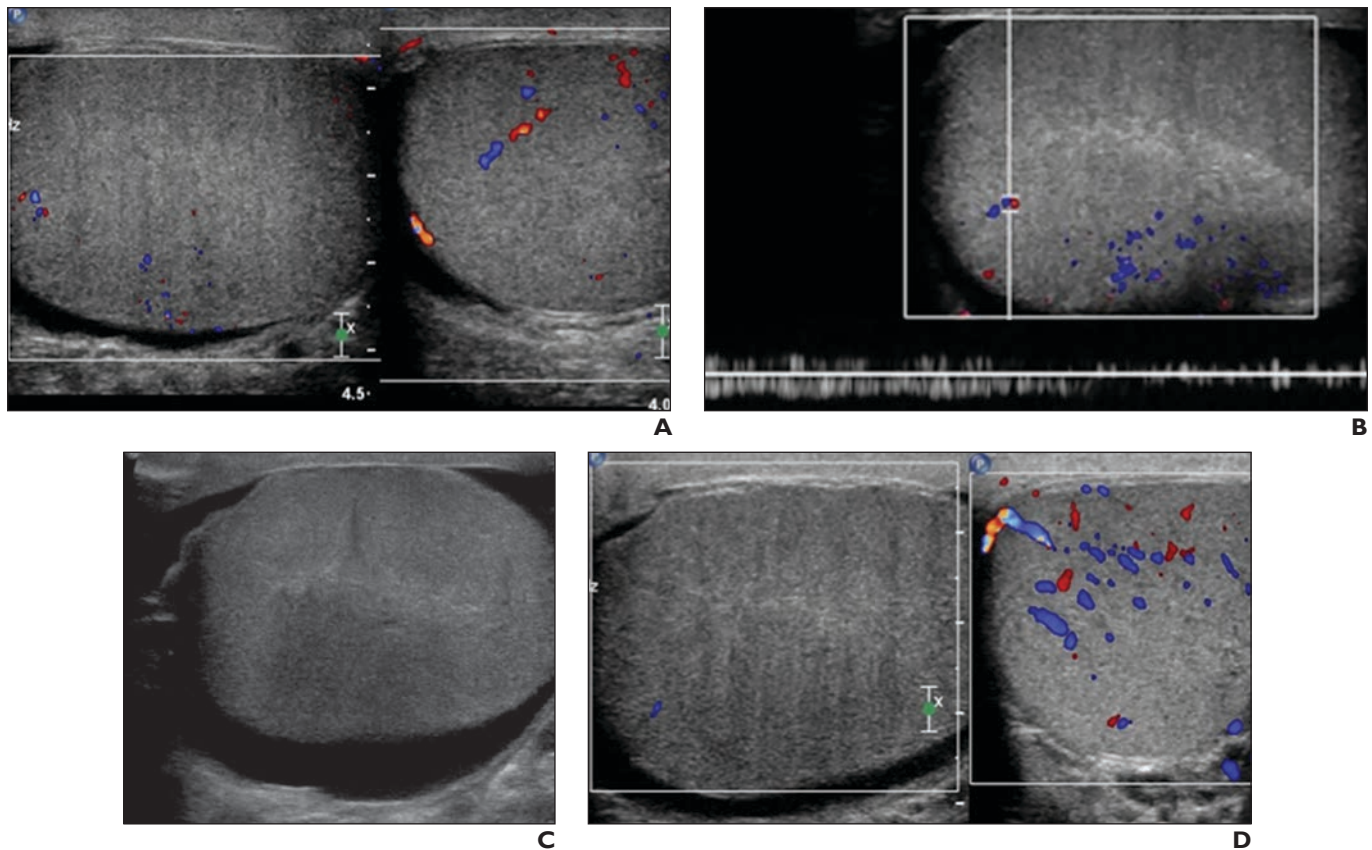


Fig. 2—47-year-old man with right testicular torsion.

A and B, Side-by-side comparison of testicle obtained with identical Doppler settings (**A**) highlights asymmetric flow with relative diminished blood flow to right testicle. Spectral Doppler tracing (**B**) shows only trace low-amplitude flow on symptomatic side. Doppler tracing was difficult to obtain and flow was diminished relative to asymptomatic left testicle.

C and D, Repeat gray-scale (**C**) and color Doppler (**D**) ultrasound images obtained 5 hours later show abnormal heterogeneous echogenicity and lack of blood flow, respectively. Torsion with nonviable right testicle was found at surgery.

Imaging of Solid Organ and Bowel Torsion

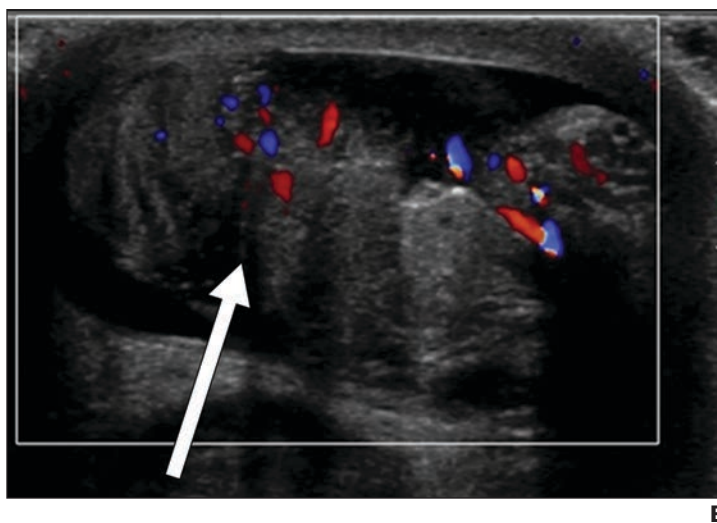
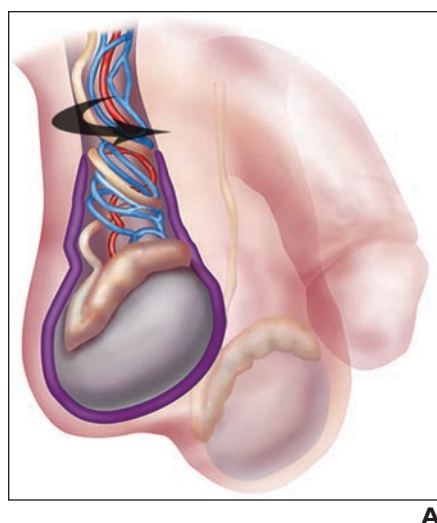


Fig. 3—27-year-old man with surgically proven right testicular torsion.

A, Drawing shows twisting of spermatic cord structures (*arrow*).

B, Sagittal color Doppler image shows ovoid heterogeneous extratesticular mass (*arrow*) representing edematous twisted intrascrotal portion of spermatic cord.

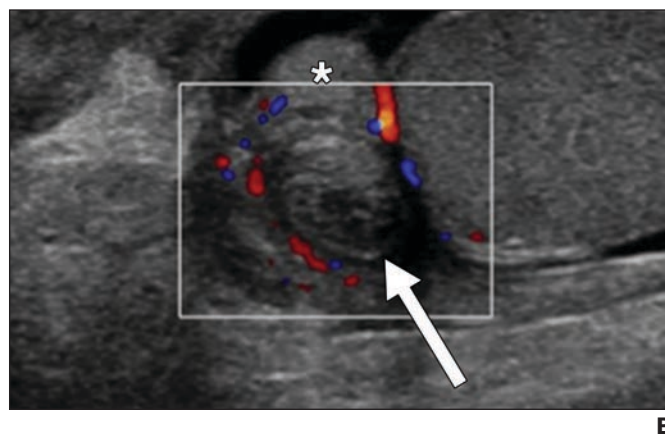
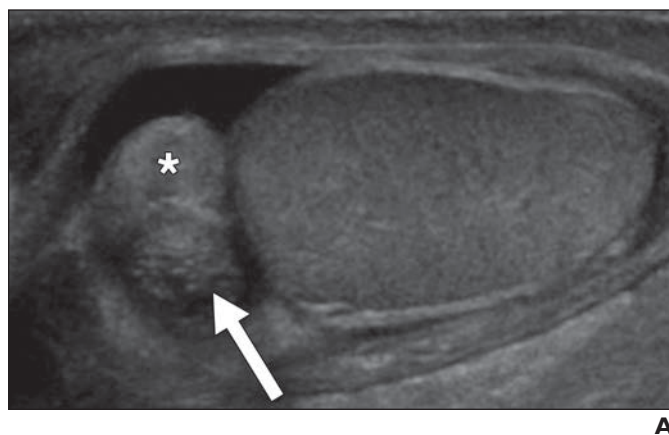


Fig. 4—12-year-old boy with acute-onset right scrotal pain secondary to torsion of appendix testis.

A and B, Sagittal gray-scale (**A**) and color Doppler (**B**) images of right epididymal head and testis show heterogeneous spherical mass (*arrow*) immediately adjacent to epididymal head (*asterisk*) with lack of internal vascularity, consistent with enlarged appendix testis. Note peripheral hyperemia in **B**.

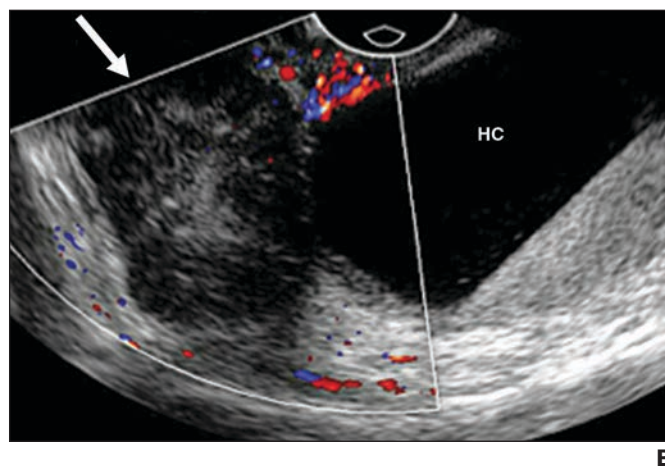
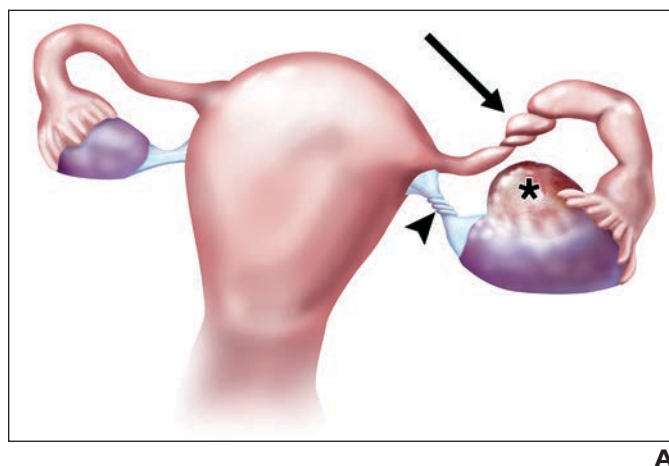
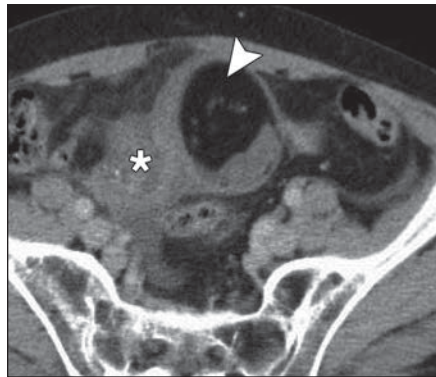


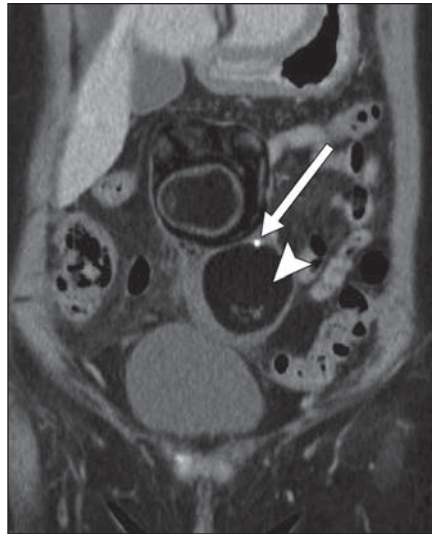
Fig. 5—Adnexal torsion.

A, Drawing shows adnexal torsion in setting of ovarian mass. Note twisting of both suspensory ligament (*arrowhead*) and fallopian tube (*arrow*). Ovarian mass (*asterisk*) predisposes to torsion by serving as lead point for ovary to rotate on its pedicle.

B, 34-year-old woman with left ovarian torsion. Color Doppler image shows enlarged ovary with heterogeneous stroma (*arrow*) and lack of arterial or venous blood flow. Notice large hemorrhagic cyst (HC) with fluid-debris level.



A



B

Fig. 6—65-year-old woman with right ovarian torsion associated with benign teratoma. **A** and **B**, Axial (**A**) and coronal (**B**) CT images show fat (arrowheads) and calcium (arrow, **B**) containing mass in right ovary. Note displacement of right ovary-mass toward midline and thickened twisted vascular pedicle (asterisk, **A**).

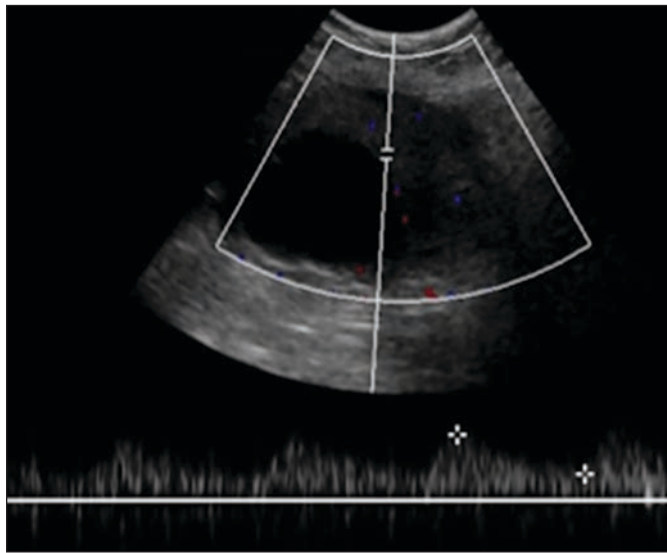
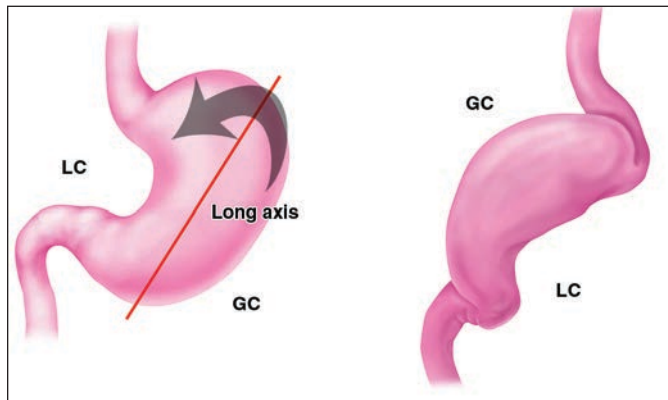
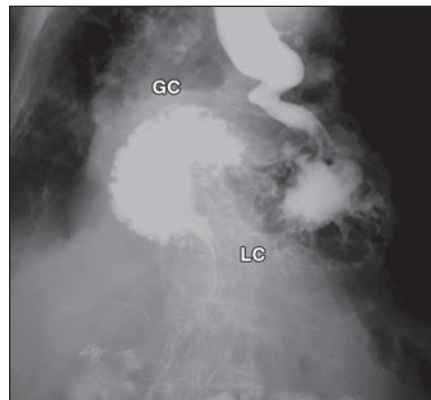


Fig. 7—27-year-old woman with surgically proven right ovarian torsion. Spectral Doppler tracing of enlarged, heterogeneous right ovary shows preservation of arterial blood flow. Venous waveform could not be obtained.



A



B

Fig. 8—78-year-old woman with organoaxial volvulus. LC = lesser curvature, GC = greater curvature. **A**, This subtype represents majority of gastric volvulus and occurs when stomach rotates about its long axis (arrow) as drawing shows. **B**, Orientation of greater curvature and lesser curvature is reversed as shown in this image from upper gastrointestinal examination.

Imaging of Solid Organ and Bowel Torsion

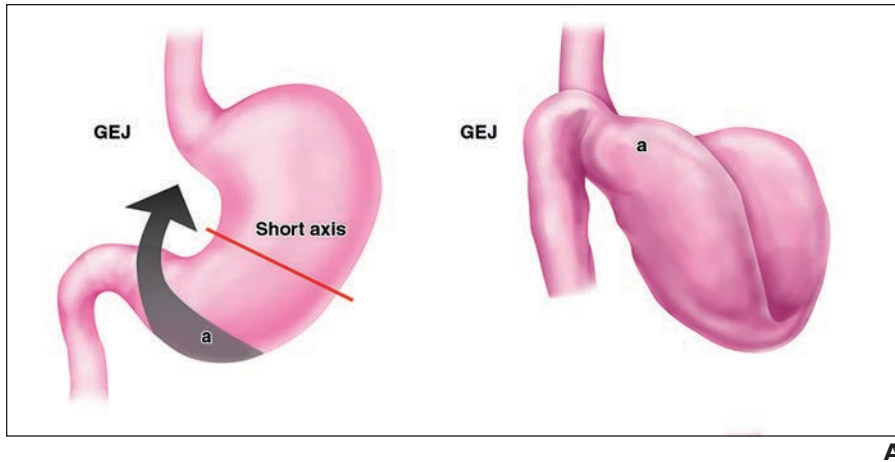


Fig. 9—71-year-old woman with mesenteroaxial volvulus.
A, This subtype occurs when there is rotation of stomach (*arrow*) about gastrohepatic ligament or short axis, with antrum (a) located above gastroesophageal junction (GEJ) as drawing shows.
B and C, Axial (**B**) and coronal (**C**) oral contrast-enhanced CT images of mesenteroaxial volvulus show antrum (a) is displaced above gas-filled distal esophagus (*arrowhead*, **B**). Twist (*arrow*) is well visualized.

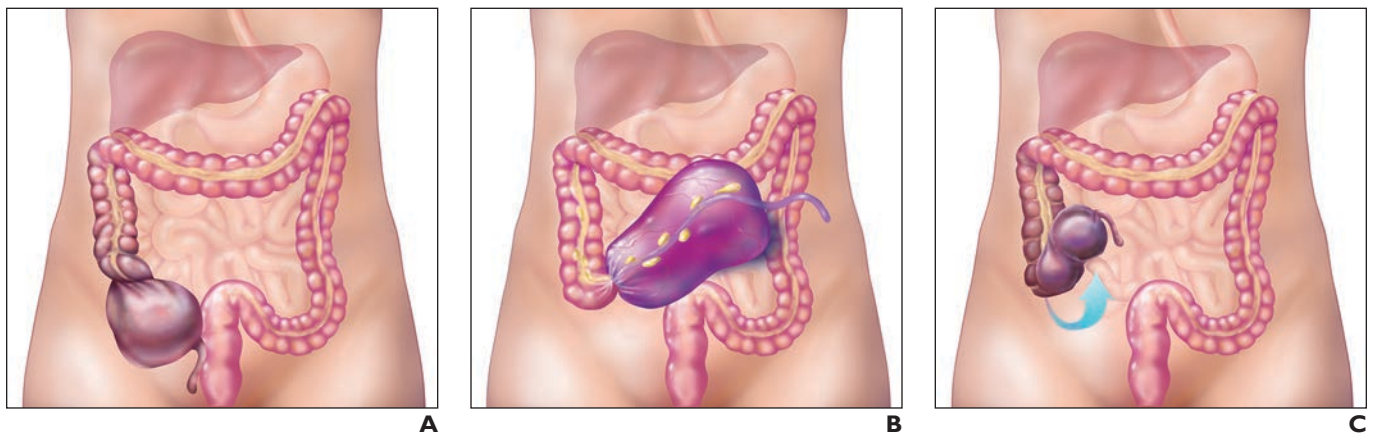
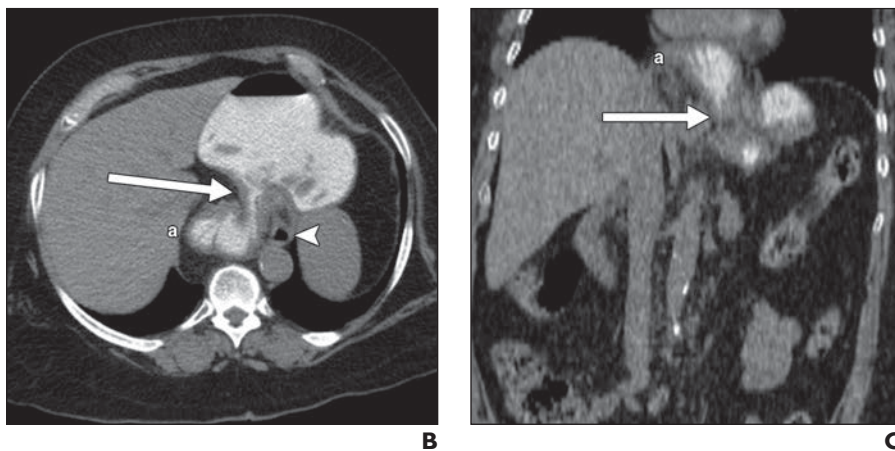


Fig. 10—Subtypes of cecal volvulus.
A–C, Drawings show axial torsion refers to twisting of cecum along its long axis (**A**). Loop-type refers to twisting in long axis of cecum with inversion (**B**). Cecal bascule is described as cranial and medial folding of cecum without twisting (*arrow*, **C**).

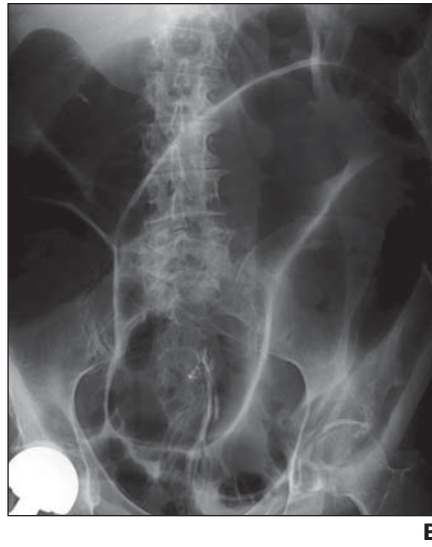
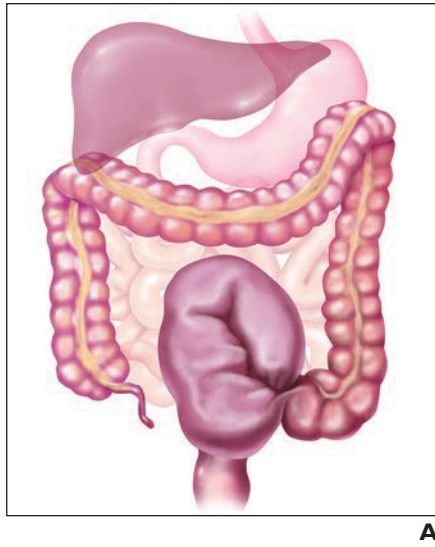


Fig. 11—83-year-old woman with sigmoid volvulus. **A** and **B**, Drawing (**A**) and abdominal radiograph (**B**) show dilated segment of sigmoid colon in midabdomen that has “coffee bean” appearance.

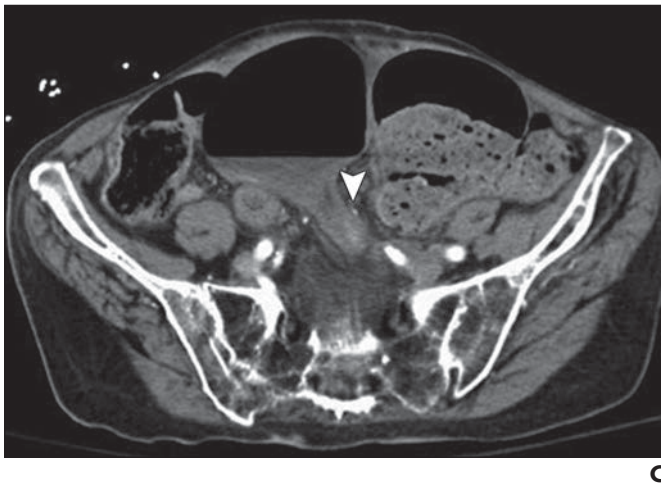
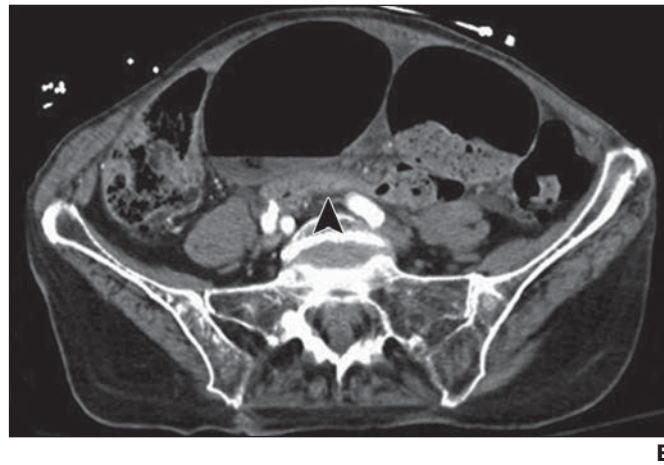
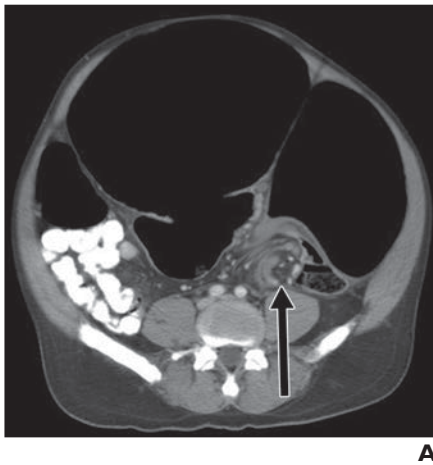


Fig. 12—Shared CT signs of colonic volvulus. **A**, Whirl sign. CT image in 74-year-old man with sigmoid volvulus shows swirling of mesentery in right lower quadrant (arrow). **B** and **C**, “X-marks-the-spot” sign. CT images in 68-year-old man with sigmoid volvulus show adjacent cranial transition point (arrowhead, **B**) and caudal transition point (arrowhead, **C**; 2 cm below **A**) traveling in opposite directions and producing X shape. (Fig. 12 continues on next page)

Imaging of Solid Organ and Bowel Torsion

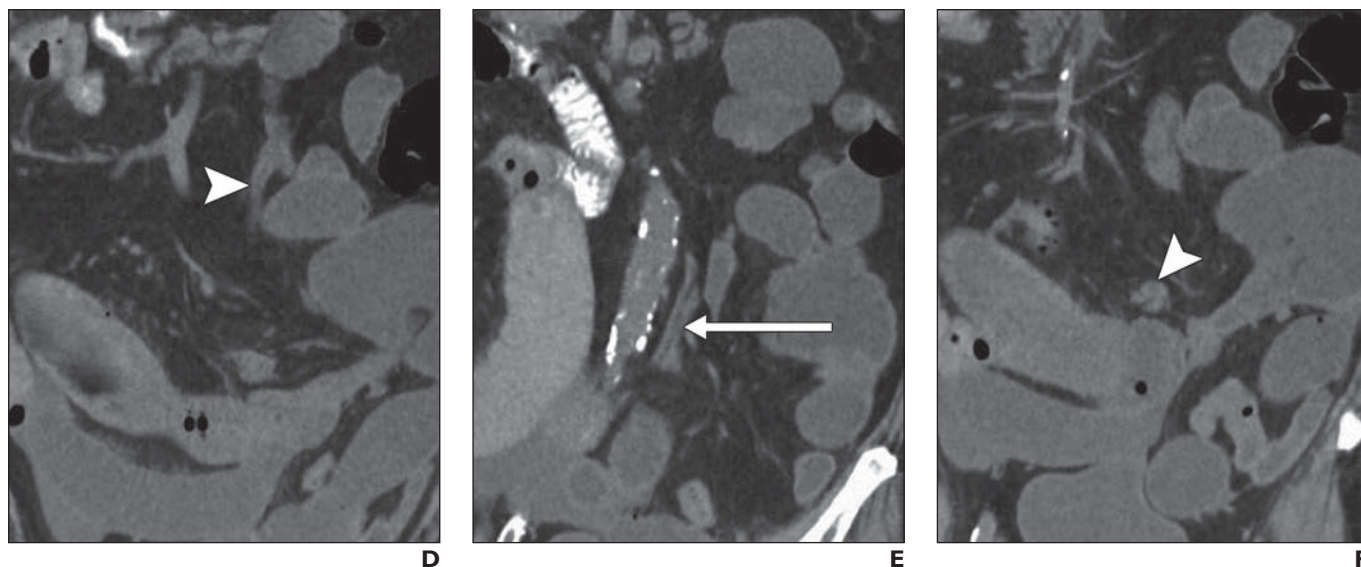


Fig. 12 (continued)—Shared CT signs of colonic volvulus.

D–F, “Split wall” sign. 59-year-old man with cecal volvulus and baseline malrotation of bowel. Invagination of mesenteric fat gives impression of “split” in single loop of twisted bowel (*arrow, E*); Notice single loop of bowel cranial and caudal (*arrowheads, D and F*) to “split wall.”

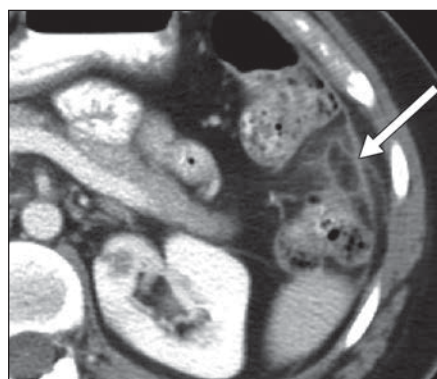


Fig. 13—CT image in 38-year-old man with epiploic appendagitis shows oval fat-containing lesion with rim of high attenuation (*arrow*) that abuts colonic wall and is surrounded by inflammatory changes.

FOR YOUR INFORMATION

This article is available for CME and Self-Assessment (SA-CME) credit that satisfies Part II requirements for maintenance of certification (MOC). To access the examination for this article, follow the prompts.